The Effect of Cross-Flow Vortex Trap Devices on the Aerodynamic Drag of Road Haulage Vehicles

Joseph Story, Isabel Vallina Garcia, Holger Babinsky
University of Cambridge, United Kingdom

Abstract

The effect of Cross-Flow Vortex Trap Devices (CVTDs) on the local flowfield and vehicle drag at a range of yaw angles has been investigated in wind tunnel experiments. The CVTD is a flow control device proposed by Bauer and Wood that aims to reduce the sensitivity of articulated road haulage vehicles to crosswinds by managing the tractor-trailer gap cross-flow. A $1/10^{th}$ scale model is used in a low speed wind tunnel at a Reynolds number of 900,000. The aerodynamic drag force is measured using a load cell connected to a rotating, raised ground plane. This research also uses tuft flow visualisation to examine the local flowfields, and pressure taps to determine trailer pressure distributions. It is found that a configuration of four 45% length CVTDs reduces the wind-averaged drag coefficient by 12%. The drag mechanisms that are responsible for the reduced drag include a lower average pressure on the trailer front face, a removal of the separation on the leeward side of the trailer due to a reduction in gap cross-flow, and an increase in pressure on the leeward side of the trailer behind the tractor-trailer gap. Furthermore, it is found that the drag reduction performance increases with CVTD length but does not vary with the number of CVTDs between one and four. These results suggest that using a single CVTD or flexible sheet of material at the centreline of the cab-gap is the most viable solution, as there is no further benefit to using multiple devices. In addition, it allows for the greatest CVTD length without impeding articulation.

1 INTRODUCTION

With an ever-increasing demand for efficient, low-emission vehicles, the road haulage industry has introduced several innovations. One particular focus for these efforts is the aerodynamic drag, due to its significant contribution to the overall vehicle drag and the relatively large scope for improvement. At speeds greater than 50mph, the Transportation Research Board and National Research Council found that the aerodynamic drag is responsible for more than 50% of the overall drag [9]. Furthermore, Van Raemdonck and Van Tooren determined that the aerodynamic drag is responsible for 39% of the fuel consumption on an average journey for a DAF XF95 type Space-cab with 3-axle trailer [12].

Castejon and Mirables identified four areas of an articulated Heavy Goods Vehicle (HGV) that are the largest contributors to the aerodynamic drag [2]. These consist of the tractor front, the tractor-trailer gap, the trailer underbody, and the trailer base. Here, we focus on the tractor-trailer gap (often referred to as the cab-gap), which is necessary to allow for cornering by articulation. Castejon and Mirables suggested that the tractor-trailer gap is responsible for 20% of the overall aerodynamic drag [2]. In particular, the tractor-trailer gap has a significant impact on vehicle drag when the gap is greater than 0.45m, with a drag increase of approximately 2% for every 0.25m of increased gap length (for a vehicle with a typical width of approximately 2.5m) [8]. It is for this reason that the maximum recommended cab-gap (defined as the distance from the trailer front face to the trailing edge of the side extender) is 0.75m (30% of the typical truck width) [9].

Ingram found that crosswinds are a particular problem in the United Kingdom due to the predominant North-South transport direction, and the prevailing East-West wind [5]. Therefore, Ingram suggested that the representative cross-

wind in the UK at motorway speeds is 5 degrees. Because of the particular importance of modelling gross effects of mean crosswind flow in wind tunnels, it is common practice to yaw the vehicle about a vertical axis relative to the oncoming flow. Ingram suggested the use of a wind-averaged drag coefficient, which scales the drag coefficient at a variety of yaw angles by the approximate time that an HGV is expected to spend at that condition [10]. HGVs are particularly susceptible to crosswinds due to their large side area. This sensitivity is exacerbated by the cab-gap because it allows a cross-flow from the windward side to the leeward side which can disrupt the overall flow field and introduce additional drag mechanisms.

As there are significant drag savings possible through cab-gap alterations and retrofit devices, understanding the flow patterns within the cab-gap both with and without flow control devices is key to capitalising on this potential. At a non-zero angle of yaw induced by a crosswind, the flow around the cab-gap is relatively complex, as shown by the expected flowfield in Figure 1. High velocity flow enters the cab-gap, impinging on the trailer front face, which creates a region of high-pressure that increases the pressure drag. The flow entering the cab-gap is part of a feature known as cab-gap cross-flow – a bulk flow from the windward to the leeward side. At the leeward side of the trailer, the flow separates, creating a region of low-pressure. Garry found that separation occurs at yaw angles above 5° [4].

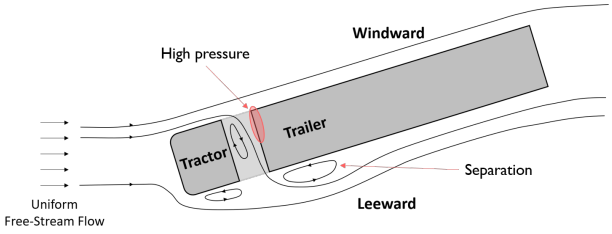

Figure 1: Expected flow patterns through the cab-gap in crosswind conditions

Since the aerodynamic drag associated with the tractor-trailer gap increases with yaw angle, many aerodynamic devices have been designed to counteract this phenomenon by reducing the gap flow, such as roof deflectors, side deflectors, side extenders, and gap seals. One such device is the Cross-Flow Vortex Trap Device (CVTD), proposed by Bauer and Wood [1]. These are vertical fins that extend forwards from the trailer front face, as shown in Figure 2. Bauer and Wood conducted on-the-road data-logging tests in North America on modern *International* day cab tractors [1]. These tractors had moderate aerodynamic shaping, including a roof deflector and side fairing, but no side extender. The *Great Dane* trailers were of equal cross-sectional area, and were separated from the tractor by a cab-gap of 1.02m. The tests were conducted over a period of 18 months, with a total of 253,600 miles covered at an average speed of 45mph. Over this period, they found that

(a) Scale model

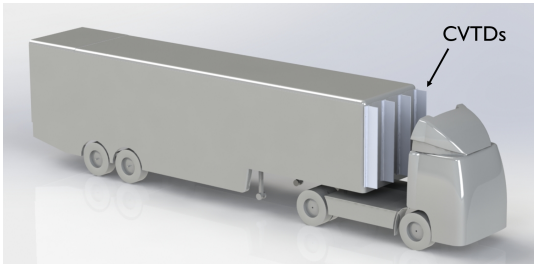

(b) CAD render

Figure 2: HGV scale model with CVTDs

the devices provide an improvement in fuel economy of 3.5 – 8.3%.

Bauer and Wood proposed the crosswind flowfield around an HGV with four CVTDs shown in Figure 3 [1]. They argued that the devices generate a vortex between each CVTD that imparts a low-pressure on the front face of the trailer, which in turn reduces the pressure drag. In addition to this, they suggested that CVTDs impede the cross-flow through the cab-gap, which in turn reduces the size of the separation bubble on the leeward side of the trailer. It is worth noting, however, that they did not provide any evidence to substantiate their hypothetical flow patterns.

The aims of this paper are therefore to test the effectiveness of CVTDs over a range of yaw angles, and to determine the mechanisms by which CVTDs reduce drag. A small parametric study is also conducted to determine the effect of device length and device number.

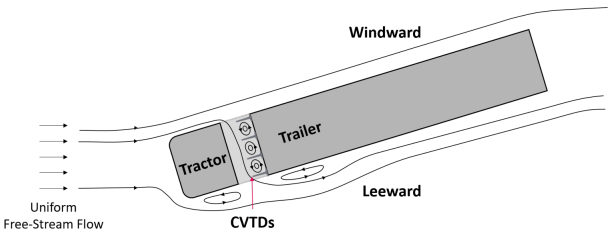

Figure 3: Expected flow patterns through the cab-gap with CVTDs in crosswind conditions

2 METHODOLOGY

2.1 Model Scale

The research is performed in the Markham low-speed wind tunnel in the Engineering Department at the University of Cambridge. The facility has a working section of 1.7 x 1.2m, with a maximum flow speed of 60m/s. An additional feature of the wind tunnel is a raised ground plane, which is used as an alternative to a rolling road to replicate the ground conditions, and hence minimise the boundary layer effect.

A $1/10^{th}$ scale model is chosen to provide a balance between Reynolds number and wind tunnel blockage, giving a Reynolds number of 900,000 (based on model width). This is greater than the critical value of 700,000 suggested by the Society of Automotive Engineers, above which the coefficient of drag remains approximately constant [10]. The wind tunnel blockage of the $1/10^{th}$ scale model ranges from 4.7% to 8.8% depending on the yaw angle of the vehicle. To account for the effect of the blockage, a correction factor is calculated using Mercker's method [11]. This method is valid for blockages of up to 15%.

The maximum full-scale cab-gap distance of 0.75m is suggested to prevent the cab-gap drag from becoming excessive [9]. However, in some situations a larger gap may offer operational advantages. In this study, we therefore wanted to explore a larger cab-gap in order to determine to what extent CVTDs could mitigate the additional drag. This offered the additional advantage that the cab-gap drag was a relatively large contribution to the overall drag, which improved the measurement accuracy. Therefore, while the actual drag magnitudes measured here may not be representative of a typical cab-gap drag, the effect of CVTDs and their relative influence on the cab-gap drag is nevertheless thought to be representative.

2.2 Load Cell Setup

The aerodynamic drag parallel to the vehicle axis is measured using the setup shown in Figure 4, which incorporates a single-ended shear beam load cell to measure the drag force. The model is mounted on front and rear sliders to ensure that the aerodynamic drag acts solely through the load cell. These sliders are incorporated into a raised ground plane that is used to minimise the boundary layer effect. To yaw the vehicle relative to the oncoming flow, the raised ground plane is connected to a rotating table with accurate markings to indicate the angle of yaw in increments of 2°. Therefore, measurements of the aerodynamic drag are taken at these increments. However, the method of calculating the wind-averaged drag coefficient specified by the Society of Automotive Engineers requires measurements at 1.7°, 2.2°, 4.7°, 5.6°, 6.8° and 7.2° [10]. Consequently, linear interpolation is used between the readings to obtain the drag coefficient at the required angles.

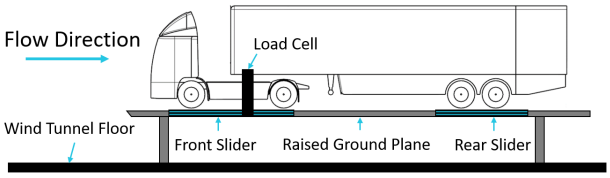

Figure 4: Wind tunnel load cell setup

Figure 5: Scale model with a complete gap seal

2.3 Complete Gap Seal

To determine the maximum drag reduction possible with cab-gap alterations, the entirety of the cab-gap is sealed off with aluminium tape as shown in Figure 5. Although such a solution is impractical because of the need of a truck to articulate, the results provide a useful metric to evaluate add-on devices. We define a device "efficiency" as the ratio of the drag reduction with a device to the maximum reduction achieved with a fully sealed cab-gap.

2.4 Model CVTDs

Model CVTDs are 3D printed and attached to the trailer front face, as shown in Figure 6. They consist of vertical plates that extend forwards from the trailer front face, as demonstrated by the model geometry shown in Figure 7(a). The geometry of the truck is defined by the length of the cab-gap (G), and the width of the trailer (W). The scale model used in this investigation has an equivalent full-scale cab-gap length of 1.4m (without side extenders). The CVTD size is defined as the ratio of the CVTD length to the length of the cab-gap (L/G), referred to in this docu-

Figure 6: 1:10th scale model with four CVTDs attached to the trailer front face

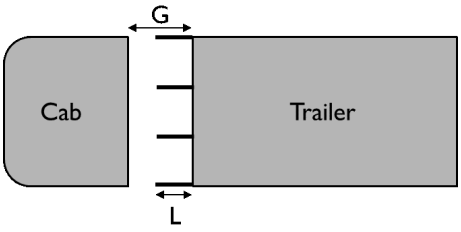

(a) Length

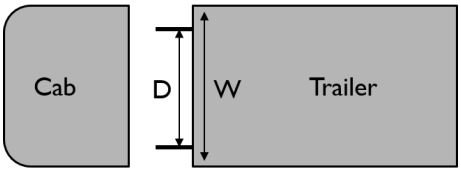

(b) Separation

Figure 7: Scale model CVTD geometry

ment as L*. In total, four CVTD variations are tested, with length ratios of 15%, 25%, 35%, and 45%.

The number of CVTDs and their length is varied. Table 1 shows all tested configurations with their geometric properties. In addition to this, tests are conducted with two CVTDs at a range of spanwise locations, as shown in Figure 7(b). The ratio of CVTD separation to the width of the trailer (D/W) is referred to in this document as D*.

2.5 Pressure Taps

The front surface of the trailer is fitted with a 3x3 grid of pressure taps, as shown in Figure 8. This arrangement is chosen so that four CVTDs can be used without covering any pressure taps. Linear interpolation is implemented between data points to obtain an approximate pressure field. Although the results have a limited resolution, they nevertheless provide a useful overview of the pressure distribution and allow for a comparison between configurations.

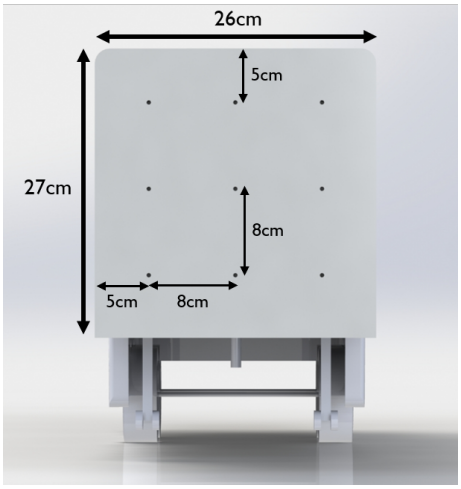

Figure 8: Trailer front pressure tap geometry

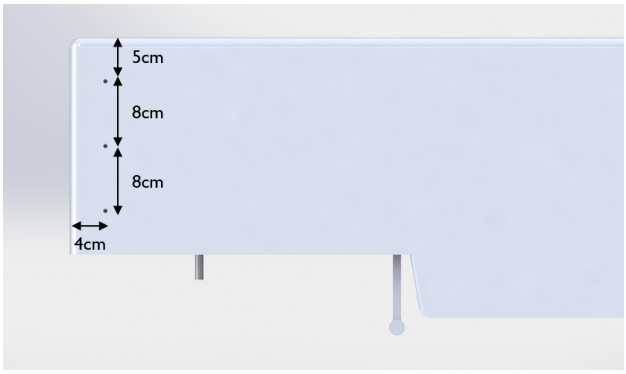

Figure 9: Trailer side pressure tap geometry

Pressure taps are also used on the leeward side of the trailer to measure the pressure in the separation bubble produced by the cab-gap. The arrangement of the side pressure taps is shown in Figure 9.

2.6 Tuft Testing

Tuft testing is used as a flow visualisation technique to find flow separation, and to determine the direction and unsteadiness of the flow. The tuft testing focuses on the tractor trailer gap, with tufts used on the leeward side of the trailer.

Configuration Name	Number of CVTDs	Size of CVTDs	Location
x1 45% CVTD	1	45%	Centre
x2 45% CVTD	2	45%	Separation: D
x4 15% CVTD	4	15%	Equally spaced
x4 25% CVTD	4	25%	Equally spaced
x4 35% CVTD	4	35%	Equally spaced
x4 45% CVTD	4	45%	Equally spaced

Table 1: List of CVTD configuration parameters

2.7 Experimental Error

The three main sources of uncertainty within this experiment are the measurements of environmental factors, the load cell reading, and the pressure tap readings. Environmental factors include the atmospheric pressure and temperature, and the wind tunnel speed, measured using a Pitot tube. These are assumed to have an uncertainty of 1%.

The load cell used in this experiment is a single-ended shear beam load cell, which initially failed to produce repeatable results of the required accuracy. However, this problem is overcome by pre-straining the load cell. There is also a very slight oscillation in the load cell reading which is solved by taking the average value over a period of 5 seconds. In addition to this, a new baseline reading is taken for each wind tunnel entry so that the corresponding drag of each configuration can be calculated as a percentage difference to this baseline reading. This repetition of the baseline reading minimises the likelihood that external factors were influencing the results. Based on the repeatability of the results and the calibration tests that were conducted, the load cell is estimated to have an uncertainty of 4%.

The final source of uncertainty is the pressure taps, which are connected to a manometer bank. The unsteady nature of the flow through the cab-gap causes the pressure at each pressure tap to oscillate. These oscillations are almost negligible on the front face of the trailer but are noticeable on the leeward side of the trailer. To compensate for this oscillation, the average of the pressure reading is taken over a period of 5 seconds. It is determined that the accuracy of the mean reading equates to a percentage error of 6% of the maximum values.

3 CVTD DRAG REDUCTION PERFORMANCE

3.1 Optimum Gap Seal

Figure 10 compares the drag coefficients of the baseline configuration at different yaw angles with the complete gap seal configuration shown in Figure 5. This shows that there are significant drag savings at all yaw angles for the gap seal configuration, increasing from 19% at 0° yaw to 25% at 8° yaw. The wind-averaged drag reduction of the complete gap seal is 20%, which agrees with the findings of Castejon and Mirables, and Janna [2,6]. It can also be seen that the curve for the complete gap seal appears to be shallower than the baseline data, suggesting that the drag savings increase with yaw angle.

3.2 Four CVTDs

The variation in percentage drag reduction with yaw angle (compared to the baseline at each yaw angle) for the complete gap seal and the configuration with four 45% length

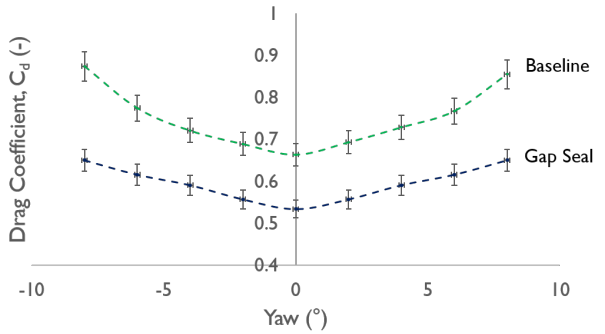

Figure 10: Comparison of the drag coefficients at a range of yaw angles between the baseline and gap seal configurations

CVTDs is shown in Figure 11. It can be seen that CVTDs have little benefit at 0° yaw. However, the CVTDs provide significant savings at higher angles of yaw, with a drag reduction of 20% at 8°, where the benefit is comparable to the complete gap seal. The wind-averaged reduction in drag coefficient for the x4 45% length CVTD configuration is 12%. This equates to an efficiency of 60% when compared to the complete gap seal, and an estimated fuel saving of 5% based on the findings of Van Raemdonck and Van Tooren [12].

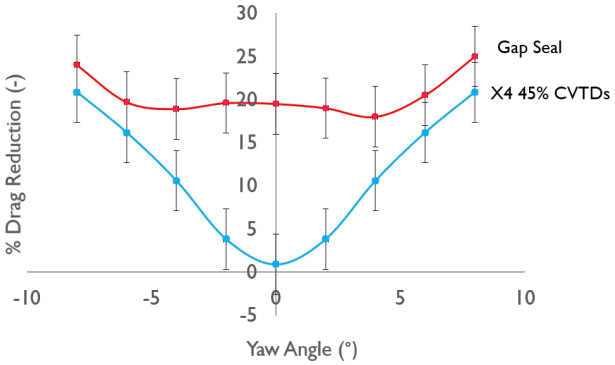

Figure 11: Variation of percentage drag reduction with yaw angle for the gap seal and CVTD configurations (compared to the baseline configuration)

4 CVTD DRAG REDUCTION MECHANISM

4.1 Trailer Front Pressure Distribution

Figure 12 compares the trailer front pressure distributions for the baseline configuration at different yaw angles, showing the static pressure in terms of the non-dimensional pressure coefficient (C_p), as shown in equation 1.

$$C_p = \frac{p - p_\infty}{p_0 - p_\infty} \tag{1}$$

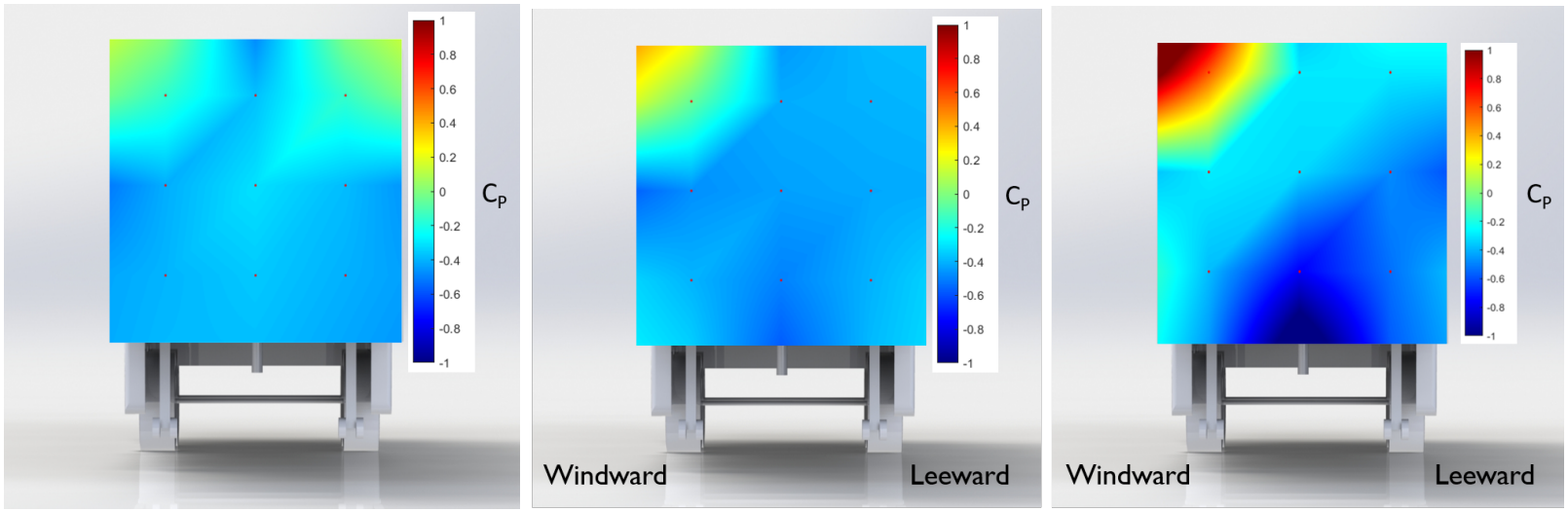

(a) 0° yaw (b) 4° yaw (c) 8° yaw

Figure 12: Trailer front pressure distributions at varying yaw angles for the baseline configuration (linear interpolation)

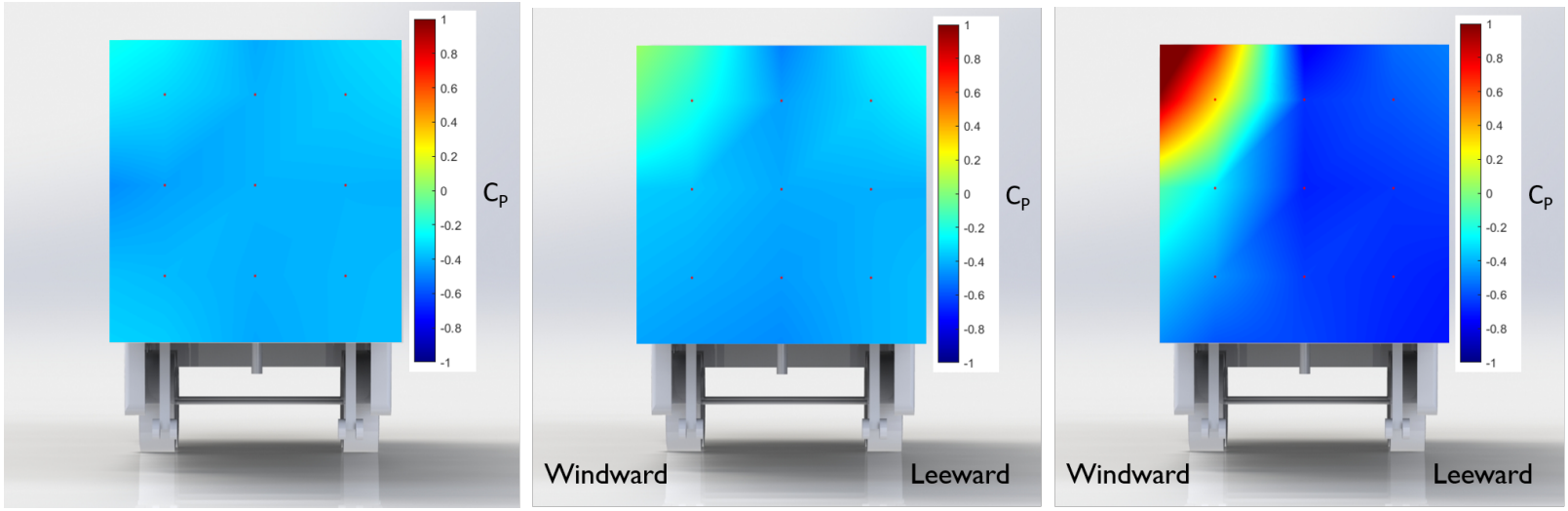

(a) 0° yaw (b) 4° yaw (c) 8° yaw

Figure 13: Trailer front pressure distributions at varying yaw angles for the x4 45% CVTD configuration (linear interpolation)

At 0° yaw (Figure 12(a)) the pressure on the trailer front face is approximately constant, although there are regions of slightly higher pressure at the top corners. This is likely because the flow is not perfectly guided over the cab-gap by the stock roof and side deflectors, allowing for the flow to impinge on the trailer front face and create localised regions of high-pressure.

At 4° yaw, there is only one high-pressure region on the windward side, as shown in Figure 12(b). At this angle, the leeward side is protected by the bulk of the cab. The average pressure coefficient in the high-pressure region appears to be slightly greater than for the 0° case, indicating that a larger portion of the trailer front face is being subjected to the high velocity oncoming flow. This is likely because yaw causes the high velocity flow to bypass the roof and side deflectors and impinge on the top windward corner of the trailer front face.

At 8° yaw, the high-pressure region is even more pronounced. Furthermore, the pressure away from the top windward corner is less uniform than in the 0° and 4° cases, perhaps indicating that the flow patterns within the cab-gap are more complex.

Figure 13 compares the trailer front pressure distribution for the x4 45% length CVTD configuration for various yaw angles. It can be seen that at 0° and 4° yaw the extent of the high-pressure region is reduced when compared to the baseline results shown in Figure 12. In contrast, at 8° yaw, the extent of the high-pressure region is approximately unchanged when CVTDs are installed. However, the pressure away from the top windward corner is lower and more uniform with CVTDs. Numerical integration of the surface pressures shows that the average pressure coefficient is reduced by 0.15 at 8° yaw when CVTDs are installed. Multiplying the change in pressure by the area of the trailer front and comparing this to the drag saving at 8° yaw suggests that improved pressure drag on the front of the trailer is responsible for 70-80% of drag reduction. It should, however, be noted that this figure is only approximate due to the limited resolution of the pressure taps. Furthermore, the results do not include the pressure distributions on the rear of the tractor or at the trailer base.

4.2 Trailer Leeward Separation

Figure 14 compares the tuft visualisation on the leeward side of the trailer at 8° yaw for the baseline configuration with the x4 45% length CVTD configuration. Figure 14(a) clearly shows a region of reversed flow, indicating that the flow has separated for the baseline configuration. Outside of the region of separation, the strong oscillation of the tufts suggests significant flow unsteadiness.

Figure 14(b) demonstrates that the use of CVTDs has a pro-

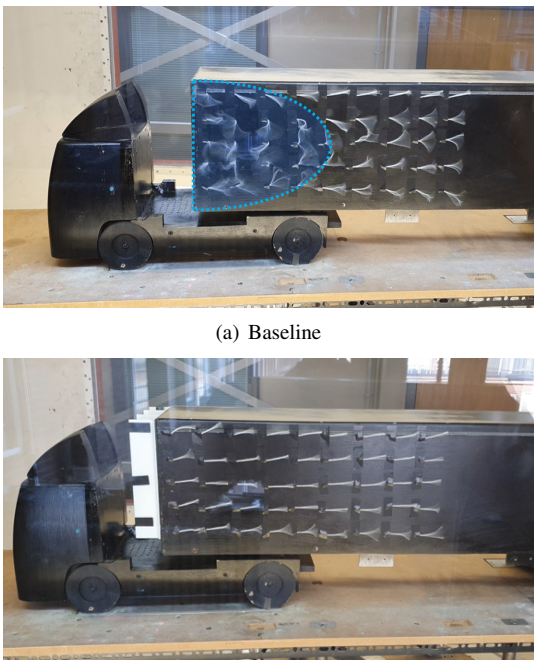

(a) Baseline

(b) x4 45% CVTD

Figure 14: Comparison of the tufts on the leeward side of the trailer for the baseline and x4 45% CVTD configuration at 8° yaw (blue shaded area indicates separation)

found effect on the leeward flow. The results show that separation does not occur when CVTDs are fitted, and that there is negligible oscillation.

Table 2 shows the static pressure coefficients at each sidewall pressure tap location (see Figure 9) for the baseline configuration and x4 45% length CVTD configuration when tested at 8° yaw. The results indicate that the presence of CVTDs significantly alleviates the low pressures observed in this area at high yaw angles. This is consistent with the absence of a large separation region, as suggested by the tuft visualisations.

Location	**Baseline**	**x4 35% CVTD**
Top	-0.858	-0.674
Middle	-0.726	-0.387
Bottom	-0.870	-0.475

Table 2: Pressure coefficients (C_p) in the separation bubble on the leeward side of the trailer (8° yaw)

Although the sidewall low-pressure region may have adverse effects on vehicle handling, it does not directly affect aerodynamic drag as it acts perpendicular to the velocity of the vehicle. However, Flynn and Kyropolous discovered that the low-pressure region on the leeward side of a trailer can extend to the trailer base, suggesting that the leeward pressure may ultimately influence the pressure drag [3]. Furthermore, alterations to the leeward pressure may also influence the pressure distribution on the trailer front

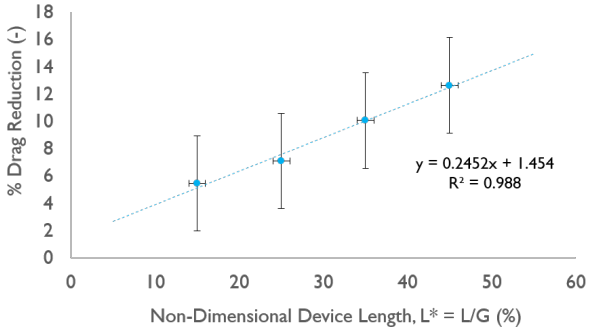

Figure 15: Reduction in wind-averaged aerodynamic drag with varying CVTD size

face.

To summarise, the main mechanisms causing the drag reductions achieved by CVTDs are a reduction in average pressure on the trailer front face, a reduction in separation on the leeward side of the trailer due to a reduced gap cross-flow, and an increase in pressure on the leeward side. Therefore, we now want to determine whether the geometry of the CVTDs (including the number, size, and separation) influences the aerodynamic drag reduction enabled by the devices.

5 EFFECT OF CVTD GEOMETRY

5.1 CVTD Size

Figure 15 shows the variation of the percentage reduction in wind-averaged drag with the non-dimensional device length (L*) when four CVTDs are fitted. The results show an approximately linear trend with larger CVTDs offering greater drag savings.

5.2 Number of CVTDs

Further tests were conducted to determine whether an increased number of CVTDs produces a greater reduction in drag. Figure 16 shows percentage drag reduction with yaw angle for configurations with one CVTD (located on the centreline), two CVTDs (located at the outer edges), and four CVTDs (equally spaced). The results demonstrate that the drag savings are approximately independent of the number of CVTDs.

Flow visualisation also suggests that there is no additional benefit to using multiple CVTDs. Figure 17 compares the trailer leeward side tufts for the x4 45% length CVTD configuration with the x1 45% length CVTD configuration. In both cases, the tufts show little oscillation. Most notably, the tufts demonstrate that the use of a single, centrally positioned CVTD (45% length) prevents the separation bub-

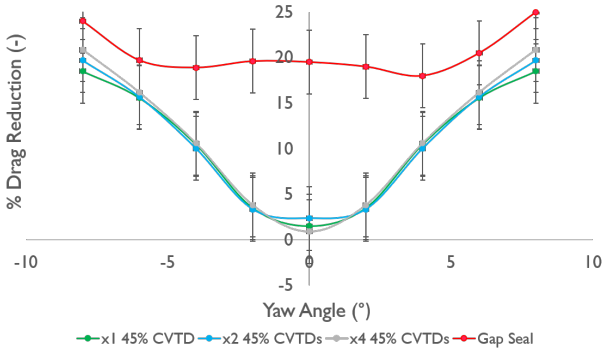

Figure 16: Reduction in drag with a varying number of CVTDs

ble from forming, indicating that increasing the number of CVTDs does not have a profound effect on the cab-gap cross-flow.

To investigate whether a different placement might offer additional benefits when using more than one device, tests with two CVTDs placed at a range of spanwise locations were conducted (as shown in the schematic of Figure 7(b)). The resulting wind-averaged drag values are shown in Figure 18. It can be seen that there is little change in the overall achievable drag saving, although there appears to be a small region where the device placement is less optimal.

The results of the tests with a varying number of CVTDs

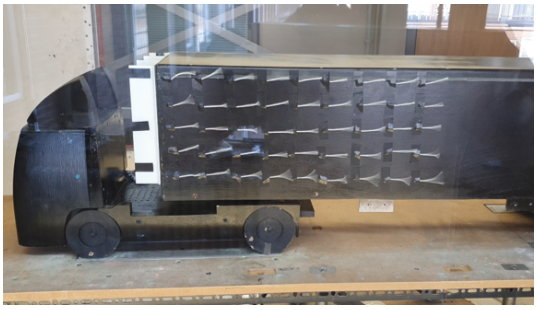

(a) x4 45% CVTD

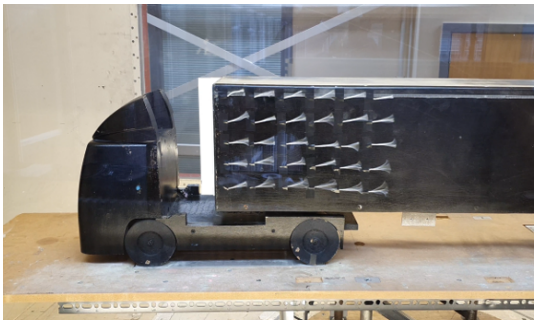

(b) x1 45% CVTD

Figure 17: Trailer leeward side tufts for different numbers of CVTDs (8° yaw)

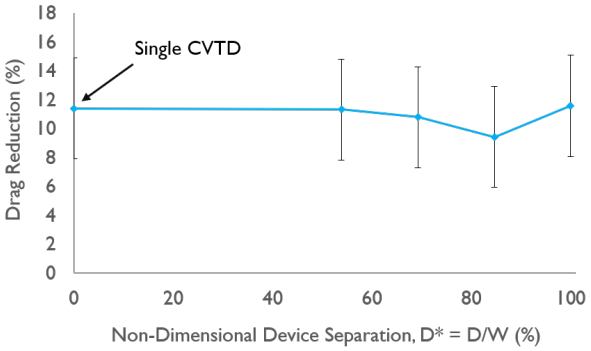

Figure 18: Reduction in wind-averaged aerodynamic drag with varying CVTD separation

and the tuft flow visualisation suggest that even a single CVTD is capable of effectively reducing the cross-flow through the cab-gap, and that additional devices do not offer any further advantage. Therefore, a viable solution would be to install a single fin at the centre of the cab-gap. This configuration allows for the greatest CVTD size without impeding articulation and would likely be easier to install. Alternatively, a flexible sheet of material could be attached to the rear of the tractor and the front of the trailer.

6 CONCLUSIONS

A simple experimental investigation into the drag control effect of CVTDs has been conducted in a low speed wind tunnel. By removing the cab-gap entirely, it was shown that the tractor-trailer gap contribution to the overall wind averaged drag is of the order of 20%. CVTDs were found to reduce the wind-averaged drag coefficient up to a maximum of 12% (compared to the baseline) when four 45% length CVTDs were used. This drag saving equates to an efficiency of 60% when compared to the maximum possible cab-gap drag savings of 20%.

The mechanisms by which the CVTDs reduce the wind averaged drag coefficient were determined to consist of a reduction in the average pressure on the trailer front face, a reduction in separation on the leeward side of the trailer due to a reduced gap cross-flow, and an increase in pressure on the leeward side of the trailer.

A positive, linear correlation between the CVTD size and the reduction in drag was observed. Furthermore, it was found that the wind averaged drag reduction is independent of the number of CVTDs between one and four devices. Based on these findings, the recommended configuration is a single fin or a flexible sheet of material placed at the centre of the cab-gap.

REFERENCES

[1] S. Bauer and R. Wood. Simple and Low Cost Aerodynamic Drag Reduction Devices for Tractor Trailer Trucks. SAE Technical Paper 2003-01-3377, 2003.

[2] L. Castejon and R. Mirables. Aerodynamic Analysis of Some Boat Tails for Heavy Vehicles. International Journal of Heavy Vehicle Systems, 19(2):115-127, 2012.

[3] H. Flynn and P. Kyropolous. Truck Aerodynamics. SAE Transactions, 70:297-308, 1962.

[4] K. Garry. A Review of Commercial Vehicle Aerodynamic Drag Reduction Techniques. Proceedings of the Institution of Mechanical Engineers, Part D: Journal of Automotive Engineering, 199(3):215-220, 1985.

[5] K. Ingram. The Wind-Averaged Drag Coefficient Applied to Heavy Goods Vehicles. Transport and Road Research Laboratory (TRRL) Supplementary Report 392, 1978.

[6] W. Janna. Introduction to Fluid Mechanics, 5th edn. CRC Press, 2015.

[7] E. Maskell. A Theory of the Blockage Effect on Bluff Bodies and Stalled Wings in a Closed Wind Tunnel. Aeronautical Research Council, 1965.

[8] National Research Council of Canada. Review of Aerodynamic Drag Reduction Devices for Heavy Trucks and Buses. Transport Canada, 2014.

[9] National Research Council. Technologies and Approaches to Reducing the Fuel Consumption of Medium- and Heavy-Duty Vehicles. The National Academies Press, 2010.

[10] Society of Automotive Engineers. SAE Wind Tunnel Test Procedure for Trucks and Buses. SAE Recommended Practice J1252, 1981.

[11] Society of Automotive Engineers. Closed-Test Section Wind Tunnel Blockage Corrections for Road Vehicles. In SAE International Congress & Exposition SP1176, Detroit, Michigan, 1996.

[12] G. Van Raemdonck and M. van Tooren. Data Acquisition of a Tractor-Trailer Combination to Register Aerodynamic Performances. The Aerodynamics of Heavy Vehicles II: Trucks, Buses, and Trains, 2nd edn. Springer, 2009.

[13] S. Watkins. Wind-Tunnel Modelling of Aerodynamics: With Emphasis on Turbulent Wind Effects on Commercial Vehicle Drag, 1990.

7 CONTACT INFORMATION

Joseph Story
University of Cambridge
jdrs3@cam.ac.uk

Holger Babinsky
University of Cambridge
hb@eng.cam.ac.uk

NOMENCLATURE

C_p	Non-dimensional pressure coefficient
D	CVTD separation
D*	Ratio of CVTD separation to trailer width (D/W)
G	Cab-gap length
L	CVTD length
L*	Ratio of CVTD length to cab-gap length (L/G)
W	Trailer width